FEASIBILITY OF THE EXPLORATION OF THE SUBSURFACE STRUCTURES OF JUPITER'S ICY MOONS BY INTERFERENCE OF JOVIAN HECTOMETRIC AND DECAMETRIC RADIATION

A. Kumamoto*, Y. Kasaba*, F. Tsuchiya*, H. Misawa*, H. Kita*, W. Puccio†, J.–E. Wahlund†, J. Bergman†, B. Cecconi‡, Y. Goto§, J. Kimura¶, and T. Kobayashi‖

Abstract

A new passive subsurface radar technique using interference patterns in the spectrum of the Jovian hectometric and decametric radiation (HOM/DAM) has been proposed, and investigated for implementation on JUICE (Jupiter Icy Moons Explorer)/ RPWI (Radio and Plasma Wave Instrument). When there occurs interference among Jovian radio waves directly from Jupiter (W1), those reflected at the ice crust surface (W2), and those reflected at the subsurface reflectors in the ice crust (W3), fine and wide interference patters can be found in the spectrum. Fine patterns are caused by interference between W1 and W2, and between W1 and W3. Wide patterns are caused by interference between W2 and W3. In order to observe these interference patterns, the receiver of JUICE/RPWI is required to resolve 100 Hz, and possess a downlink spectra with a frequency range of 2 MHz and resolution of 1 kHz. Based on the calculation of the attenuation rate of the radio waves in the ice from 80 K (surface) to 250 K (just above the subsurface ocean), the intensity of the subsurface echo was estimated. The radar waves are expected to reach just above the ice crust/liquid ocean boundary. However, due to extremely high attenuation, it is difficult to detect the echoes from ice crust/liquid ocean boundary. In order to apply the new passive subsurface radar methods, the duration of the coherence of the Jovian radio wave should be long enough (>3.3 ms if spacecraft's altitude is 500 km).

* *Tohoku University, Sendai, Japan*
† *Swedish Institute of Space Physics, Uppsala, Sweden*
‡ *LESIA, Observatoire de Paris, Meudon, France*
§ *Kanazawa University, Kanazawa, Japan*
¶ *Osaka University, Toyonaka, Japan*
‖ *Korea Institute of Geoscience and Mineral Resources, Daejeon, Korea*

1 Introduction

Icy moons of Jupiter are important targets in future explorations, not only from the viewpoint of origin and evolution of the icy moons, but also from astrobiology. Several feasibility studies have already been performed for probing subsurface structures of the ice crust and the liquid ocean below it by using space-borne radar [Chyba et al., 1998; Bruzzone et al., 2011]. Although the radar is a powerful tool for subsurface probing, Jovian hectometric and decametric (HOM/DAM) emissions in a frequency range from several MHz to 40 MHz become strong noise to the radar observations especially in the sub-Jovian hemisphere of the icy moons. On the other hand, Romero–Wolf et al. [2015] proposed to apply an interferometric reflectometry technique for subsurface probing of the icy moons by using the strong Jovian radio waves. In their method, waveforms of subsurface echoes of Jovian radio waves could be detected by applying auto correlation analysis to the observed waveform, which includes Jovian decametric radiations directly from Jupiter, and those reflected on/in the ice crust of the Jovian moons. Evaluations of the SNR in passive sounding observations using JUICE (Jupiter Icy Moons Explorer)/ RIME (Radar for Icy Moon Exploration) and Europa Clipper/REASON (Radar for Europa Assessment and Sounding: Ocean to Near-surface) were also performed by Schroeder et al. [2016].

In this paper, another new subsurface probing method of Ganymede's ice crust is proposed by using Jovian HOM/DAM emissions. The idea came from the interference patterns found in the spectrogram of Earth's auroral kilometric radiation (AKR) measured by SELENE (Kaguya) [Ono et al., 2010]. They are caused by the interference between the AKR directly from Earth and AKR reflected at the lunar surface. The SELENE spacecraft moved around the terrestrial Moon at an altitude of about 100 km, thereby changing the ray path lengths of direct AKR and reflected AKR. Thus, we can see the change of phase difference between two AKR waves as interference patterns in the spectrogram. The phase difference can also be changed by the plasma surrounding the Moon. Goto et al. [2011] discussed the feasibility of the detection of the Moon's ionosphere using the AKR interference. In order to perform the passive radar observations in this method with JUICE/RPWI (Radio and Plasma Wave Instrument), we are planning to implement the firmware and onboard software for this observation. The configurations of interference among the Jovian radio waves directly from Jupiter, and those reflected at the surface/subsurface structures on/in the ice crust of the moons are described in Section 2. The maximum detection depth of the subsurface echo is estimated in Section 3. Typical interference patterns to be found in the spectrum of Jovian radio waves are shown in Section 4. The discussion of coherence of Jovian radio waves and requirements of the receiver of JUICE/RPWI are given in Section 5.

2 Configurations of interference

The interference of a Jovian radio wave in the vicinity of the moon's surface can be modeled as follows: We assume that (a) the source of the Jovian radio wave is far from the spacecraft in orbit around the moon. The radio wave therefore arrives as a plane wave. (b) As shown in Figure 1, the spacecraft observes not only the radio waves directly

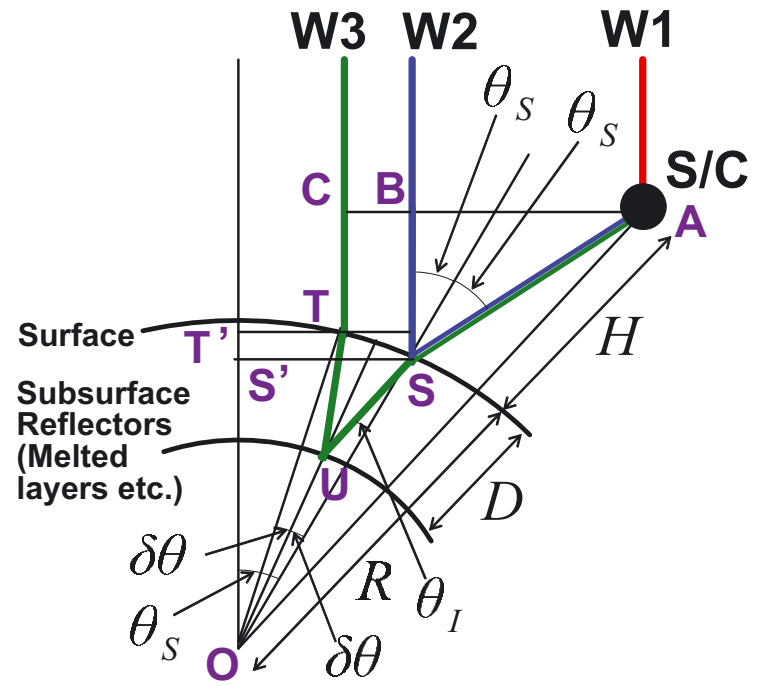

Figure 1: Jovian radio waves directly from Jupiter (W1), reflected at the moon's surface (W2), and reflected at the subsurface reflectors (W3).

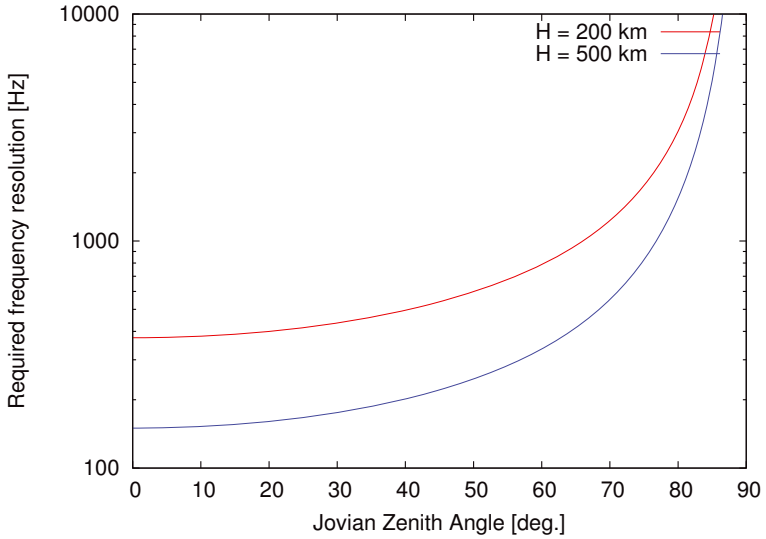

Figure 2: Required frequency resolution $\Delta f/2$ as a function of θ_S.

from Jupiter (called "W1" hereafter) but also those reflected at the moon's surface (called "W2" hereafter), and those reflected at the subsurface reflector below the moon's surface (called "W3" hereafter). Because light path lengths of W2 and W3 are similar, and much longer than that of W1, we can see fine patterns in the spectrogram of Jovian radio waves due to W1–W2 and W1–W3 interference and wide patterns due to W2–W3 interference. In order to determine the depth of the subsurface structures, the receiver has to resolve

the fine interference patterns and cover a wider frequency range than the wide interference patterns.

The bandwidth of the fine interference patterns can be estimated by simply assuming the interference between W1 and W2. The difference of the W1 and W2 path lengths, ΔL_S is geometrically given by

$$\Delta L_S = \overline{AS} + \overline{SB} = 2R\cos^3\theta_S \left(\sqrt{1 + \frac{2HR + H^2}{R^2\cos^2\theta_S}} - 1 \right) \tag{1}$$

where R is radius of Ganymede (2,631 km), H is spacecraft's altitude from the moon's surface, and θ_S is Jovian zenith angle at the reflection point on the moon's surface, or the incident angle of Jovian radio waves. The condition of the intensification (i.e. constructive interference) of interfered waves is given by $\Delta\phi = 2\pi n = 2\pi\Delta L_S/\lambda + \Theta$, where λ is the wavelength, and n is an integer. Θ is 0 or π depending on θ_S and propagation modes (Transverse Electric (TE) and Transverse Magnetic (TM) modes). The frequency of the interference patterns in the spectrogram is therefore given by

$$f_n = c \left\{ 2R\cos^3\theta_S \left(\sqrt{1 + \frac{2HR + H^2}{R^2\cos^2\theta_S}} - 1 \right) \right\}^{-1} \left(n + \frac{\Theta}{2} \right) \tag{2}$$

where c is the speed of light in vacuum. In order to resolve the interference patterns, the frequency resolution of the receiver should be better than $\Delta f/2 = (f_{n+1} - f_n)/2$. In Figure 2, $\Delta f/2$ is shown as a function of θ_S. For example, in order to observe interference patterns in all areas of the moon's surface from the spacecraft at an altitude of 500 km, the frequency resolution of the receiver should be better than 100 Hz.

The wide interference patterns in the spectrogram can be estimated as follows: We assume that there are space, an ice layer with the thickness of D, and a subsurface reflector such as a partial melt layer. The coordinate system is defined as follows: the z-axis is in the zenith direction at the reflection point on the moon's surface. the x-axis is in the incident plane. The complex amplitude of the electric field of the interfered waves are given by

$$\begin{aligned} E_x &= \{1 - R_{TM}(\theta_S, 1, n_I)\exp(2\pi i\Delta L_S/\lambda) - T_{TM}(\theta_S, 1, n_I)R_{TM}(\theta_I, n_I, n_W) \\ &\quad \times T_{TM}(\theta_I, n_I, 1)A_I\exp(2\pi i(\Delta L'_S + n_I\Delta L'_I)/\lambda)\}E_J\cos\theta_S \end{aligned} \tag{3}$$

$$\begin{aligned} E_y &= \{1 + R_{TE}(\theta_S, 1, n_I)\exp(2\pi i\Delta L_S/\lambda) + T_{TE}(\theta_S, 1, n_I)R_{TE}(\theta_I, n_I, n_W) \\ &\quad \times T_{TE}(\theta_I, n_I, 1)A_I\exp(2\pi i(\Delta L'_S + n_I\Delta L'_I)/\lambda)\}(\pm iE_J) \end{aligned} \tag{4}$$

$$\begin{aligned} E_z &= \{1 + R_{TM}(\theta_S, 1, n_I)\exp(2\pi i(\Delta L_S/\lambda) + T_{TM}(\theta_S, 1, n_I)R_{TM}(\theta_I, n_I, n_W) \\ &\quad \times T_{TM}(\theta_I, n_I, 1)A_I\exp(2\pi i(\Delta L'_S + n_I\Delta L'_I)/\lambda)\}E_J\sin\theta_S \end{aligned} \tag{5}$$

where E_j is the complex amplitude of Jovian radio waves directly from Jupiter with circular polarization, $R_{TM}(\theta_1, n_1, n_2)$ and $R_{TE}(\theta_1, n_1, n_2)$ are the Fresnel reflectance of TM and TE mode waves with incident angle θ_1 from a medium with the refractive index

n_1 to a medium with the refractive index n_2, $T_{TM}(\theta_1, n_1, n_2)$ and $T_{TE}(\theta_1, n_1, n_2)$ are Fresnel transmittance of TM and TE mode waves with incident angle θ_1 from a medium with n_1 to a medium with n_2; θ_S, θ_I, and θ_W are incident/reflection/transmission angles in space, ice, and liquid water, n_I and n_W are refractive indices of ice and liquid water, ΔL_S is the path length difference between W1 and W2 in space, $\Delta L'_S$ and $\Delta L'_I$ are path length differences between W1 and W3 in space and ice, respectively. Using the relative permittivity of space, ice, and liquid water, 1, 3, and 87, respectively, we can calculate reflectance and transmittance of TM and TE mode waves. ΔL_S is given by Equation (1). $\Delta L'_S$ and $\Delta L'_I$ are also geometrically given by

$$\begin{aligned} \Delta L'_S &= \overline{AS} + \overline{TC} = \overline{AS} + \overline{SB} - (\overline{OT'} - \overline{OS'}) \\ &= 2R\cos^3\theta_S \left(\sqrt{1 + \frac{2RH + H^2}{R^2\cos^2\theta_s}} - 1 \right) - (R\cos(\theta_S - 2\delta\theta) - R\cos\theta_S) \end{aligned} \quad (6)$$

$$\Delta L'_I = \overline{SU} + \overline{UT} = 2R\cos\theta_I \left(1 - \sqrt{1 - \frac{2RD - D^2}{R^2\cos^2\theta_I}} \right) \quad (7)$$

where $\delta\theta$ is obtained from $(\sin\delta\theta)/(\Delta L'_I/2) = (\sin\theta_I)/(R - D)$. The total two–way attenuation A_I was estimated by

$$A_I = 10^{-\frac{2}{20}\int_0^{D/\cos\theta_I} \alpha_I(z)dz}, \quad (8)$$

where $\alpha_I(z)$ is the one–way attenuation rate in dB/m as a function of depth z, and D is the depth of the partial melt layer. α_I is given by

$$\alpha_I[\mathrm{dB/m}] = 0.0455 \times 10^{-6}(\epsilon_{rI})^{1/2} f[\mathrm{Hz}] \tan\delta_I = 818(\epsilon_{rI})^{-1/2}\sigma_I, \quad (9)$$

where ϵ_{rI} is the relative permittivity of ice, f is the frequency in Hz, $\tan\delta_I$ is the loss tangent of ice, and σ_I is the electrical conductivity of ice in S/m [Evans, 1965; Chyba et al., 1998; Moore, 2000]. According to Fujita et al. [2000], $\tan\delta_I$ is proportional to $1/f$ in a frequency range below 100 MHz in temperature ranges above 190 K. Therefore, as discussed in several studies [Evans, 1965; Chyba et al., 1998; Moore, 2000; Fujita et al., 2000; Bruzzone et al., 2011], the electrical conductivity of ice σ_I does not depend on the frequency in these frequency and temperature ranges. Since the temperature distribution below the surface is unknown, we have to assume some temperature distribution models in order to estimate the two–way total attenuation in the ice layer. The total thickness of the ice crust of Ganymede was suggested to be larger than 150 km based on observations with Galileo's magnetometer [Kivelson et al., 2002]. In order to estimate the attenuation rate in the ice crust, some models were assumed by Moore [2000]. In their models, the temperature at the surface is 80 K and increases to 270 K at the boundary between the ice crust and liquid ocean. In recent studies, the temperature at the boundary is estimated to be 250 K due to the high pressure of 200 MPa [Vance et al., 2014]. In this study we assume a linear increase of the temperature from 80 K to 250 K below Ganymede's surface. The electrical conductivity and attenuation are derived from the temperature by using equations for a pressure of 0.1 GPa indicated in Chyba et al. [1998]. According to Hubmann [1978], the electrical conductivity of the ice increases with increase of pressure up to 150 MPa. Thus, the attenuation estimated in this study will be less than actual one especially around the ice crust/liquid ocean boundary.

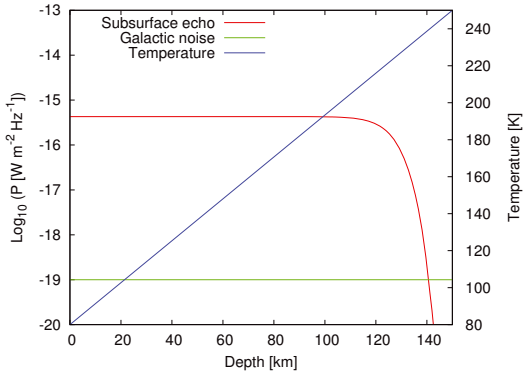

Figure 3: Intensity of subsurface echoes (red) and galactic noise (green) at Ganymede as a function of subsurface reflector depth. Blue line indicates temperature.

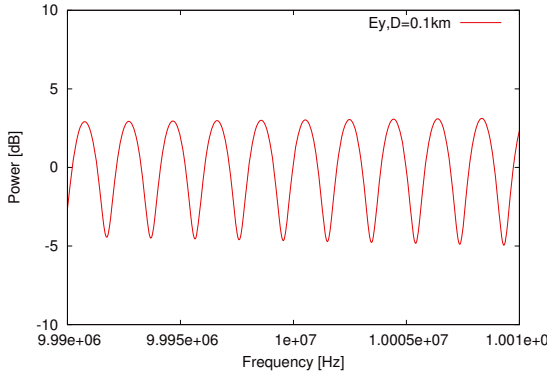

Figure 4: Expected fine interference patterns of E_y in the spectrum observed when the depth of the melted layer is 0.1 km.

3 Maximum detection depth

The maximum detection depth of the melted water in the ice crust can be estimated based on the ratio of the subsurface echo level to the galactic noise level. For a simple estimation, we assume an incident angle of 0°, in which case $R = R_{TM} = R_{TE}$, and $T = T_{TM} = T_{TE}$. The signal–to–noise ratio is given as a function of the depth of the subsurface melted layer D by $SNR(D) = |T(0, 1, n_I)R(0, n_I, n_W)T(0, n_I, 1)A_I(D)|^2 P_J/P_{GN}$ for an incident angle of 0°, where P_J is the intensity of Jovian radio waves, and P_{GN} is the intensity of galactic noise. The subsurface structures in the depth range where $SNR(D) > 1$ are expected to be detectable using this method. The intensities of Jovian radio waves at Ganymede, and the galactic noise at 1–40 MHz are 3×10^{-15} W m^{-2}Hz^{-1}, and 10^{-19} W m^{-2}Hz^{-1}, respectively [Cecconi et al., 2012]. The intensity of subsurface echoes and the galactic noise at Ganymede are shown in Figure 3. The subsurface echoes from the depth range where the temperature is below 220 K, or above 120 km in Ganymede, are expected to be detected by this method.

4 Expected interference patterns in the spectrum

Typical expected interference patterns in the spectrum observed with subsurface reflectors at depths of 1 km and 0.1 km are shown in Figures 4–6. In these calculations the location of spacecraft is at an altitude of 500 km above the point with $\theta = 75°$. The fine interference patterns are shown in Figure 4. In addition, as shown in Figures 5 and 6, the interval of the interference patterns in the spectrum changes depending on $1/D$. As reported in previous studies [Leblanc, 1981], we can expect that the bandwidth of Jovian radio waves is wider than 2 MHz in most cases.

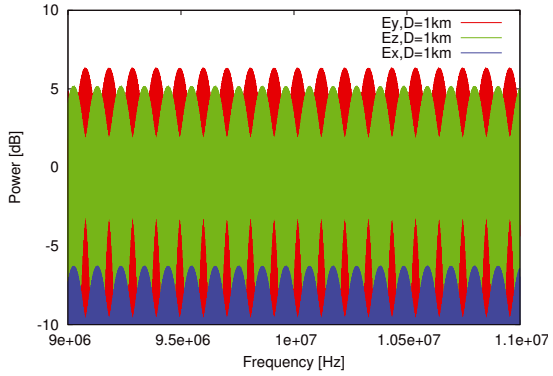

Figure 5: Expected wide interference patterns of E_y (red), E_z (green), and E_x (blue) in the spectrum observed when the depth of the melted layer is 1 km.

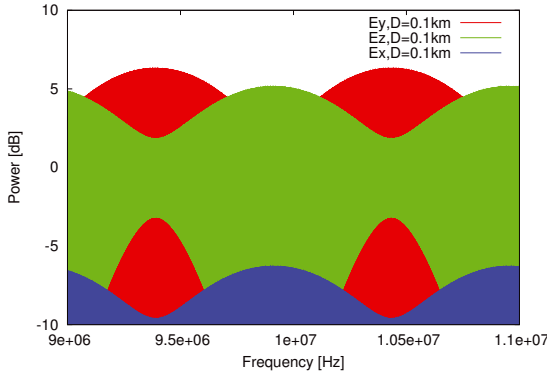

Figure 6: Expected wide interference patterns of E_y (red), E_z (green), and E_x (blue) in the spectrum observed when the depth of the melted layer is 0.1 km.

5 Discussion and summary

Based on the estimations shown in Sections 2, 3, and 4, the requirements to JUICE/RPWI are summarized as follows:

1. In order to resolve the narrow interference patterns caused by W1–W2 and W1–W3 interference, the bandwidth of the receiver has to be less than 100 Hz (assumed spacecraft altitude: 500 km) (Figures 2 and 4).

2. In order to observe the wide interference patterns caused by the W2–W3 interference, the downlink spectrum from the receiver has to cover the frequency range of several MHz with enough resolution. If we are going to cover the depth range of the subsurface reflectors in the ice crust from 0.1 km to 150 km, we have to downlink a spectrum with a frequency range of 2 MHz with a resolution of 1 kHz (assumed Jovian zenith angle: $\theta = 75°$; Equations (3)–(5), Figures 5 and 6).

3. The maximum detection depth of the passive radar at the icy moons is highly dependent on their internal temperature structures. The radio waves are expected to reach just above the boundary between the ice crust and liquid ocean. However, due to extremely high attenuation, it is difficult to assure the detection of the echoes from the ice crust/liquid ocean boundary. (Assumptions: 80 K at surface, and 250 K at ice crust/liquid ocean boundary; Figure 3).

Telemetry rate for downlink of the interference patterns is not expected to be too high, but as large as that of the spectrum monitor at the lowest rate. If further reduction of the data rate is needed, we will perform passive subsurface radar operation only when we can expect a high occurrence probability of Jovian HOM/DAM based on previous reports [e.g. Imai et al., 2011]. In principle, it is possible to demonstrate this method also by numerical simulations, observations, and laboratory experiments. Subsurface soundings

of the ice layers in Antarctica using VHF transmitter and receiver from an aircraft were reported by several studies [Siegert et al., 1998]. In laboratory experiments we need a reflector whose size is much larger than the wavelength. So we should use radio waves in the UHF range, in which the wavelength is in a range of 0.1–1 m, and prepare a reflector with a size of several meters. Ground penetrating radars (GPR) operated in the UHF range are widely used for imaging of buried rocks, soils, and artificial objects. The airborne radars and GPR mentioned above were designed for using standard radar technique. For the purpose of demonstration of the subsurface sounding proposed in this study, the radar system should be modified to transmit broad-band pulses with a long duration and measure the spectrum of received radio waves.

The evaluation of the effects of Ganymede's ionospheric plasma and roughness of its surface were not done in this study, and are deferred to future studies. The roughness of the surface would cause a decrease of the radio wave intensity at reflections and transmission. However, we can also expect that roughness doesn't affect the interference because phase variation due to the roughness is incoherent. In observations of one electric field component, identification of the interference patterns could be difficult due to overlapping of the Faraday fringes caused by dense plasma of the Io plasma torus and the moon's ionosphere on the ray path of Jovian HOM/DAM. The frequency width of a Faraday fringe is a few to several hundreds kHz [Tokumaru et al., 1995]. However, this difficulty can be avoided by polarization or cross-spectrum measurements of two or three electric field components.

In addition, we have to point out that the duration of the coherent emission is important in passive radar observations. If the spacecraft's altitude is 500 km, the arrival time of the Jovian radio waves reflected at the moon's surface is delayed 3.3 ms with respect to those directly from Jupiter. If the coherency of the emissions is kept for more than 3.3 ms, we can expect occurrence of interference patterns in the spectrum. However, if the coherency is kept for less than 3.3 ms, we cannot expect interference between direct wave and reflected wave delayed for 3.3 ms from the direct wave. We can also point out that another passive radar method with auto correlation analysis [Romero–Wolf et al., 2015] depends differently on the duration of the coherency. If the coherency is kept for more than 3.3 ms, direct waves shows high correlation not only with their own echoes but also with the direct waves after 3.3 ms, and we cannot determine which are subsurface echoes in the observed waveform. If the coherency is kept for less than 3.3 ms, the direct waves after 3.3 ms shows low correlations, and we can easily find out subsurface echoes with high correlation. It was reported by several studies that the duration of the coherence of S-bursts are 10–100 μs [Carr and Reyes, 1999; Carr, 2001]. On the other hand, in the case of AKR interference observed by SELENE, the spacecraft's altitude was 100 km. So the duration of the coherency of AKR was estimated to be longer than 0.67 ms. Investigations of Jovian HOM/DAM including other emissions than S-burst based on ground-based observation will be possible and important in further feasibility studies.

Acknowledgments. This study is supported by JSPS and MAEDI under the Japan–France Integral Action Program (SAKURA). The Editors thank Charles Higgins and one anonymous reviewer for their help in evaluating this paper.

References

Bruzzone, L., G. Alberti, C. Catallo, A. Ferro, W. Kofman, and R. Orosei, Subsurface radar soundings of the Jovian moon Ganymede, *Proc. IEEE*, **99(5)**, 837–857, doi:10.1109/JPROC.2011.2108990, 2011.

Carr, T. D., and F. Reyes, Microstructure of Jovian decametric S bursts, *J. Geophys. Res.*, **104**, 25127–25141, 1999.

Carr, T. D., New clues from the microstructure of Jupiter's S-bursts, in *Planetary Radio Emissions V*, edited by H. O. Rucker, M. L. Kaiser, and Y. Leblanc, Austrian Academy of Science Press, Vienna, 77–89, 2001.

Cecconi, B., S. Hess, A. Herique, M. R. Santovito, D. Santos–Costa, P. Zarka, G. Alberti, D. Blankenship, J.–L. Bougeret, L. Bruzzone, and W. Kofman, Natural radio emission of Jupiter as interferences for radar investigations of the icy satellites of Jupiter, *Planet. Space Sci.*, **61**, 32–45, doi:10.1016/j.pss.2011.06.012, 2012.

Chyba, C. F., S. J. Ostro, and B. C. Edwards, Radar detectability of a subsurface ocean on Europa, *Icarus*, **134**, 292–302, doi:10.1006/icar.1998.5961, 1998.

Evans, S., Dielectric properties of ice and snow – A review, *J. Glaciol.*, **5**, 773–792, 1965.

Fujita, S., T. Matsuoka, T. Ishida, K. Matsuoka, and S. Mae, A summary of the complex dielectric permittivity of ice in the megahertz range and its applications for radar sounding of polar ice sheets, *Physics of Ice Core Records*, 185–212, 2000.

Goto, Y., T. Fujimoto, Y. Kasahara, A. Kumamoto, and T. Ono, Lunar ionosphere exploration method using auroral kilometric radiation, *Earth Planets Space*, **63**, 47–56, doi:10.1029/JA082i013p01825, 2011.

Hubmann, M., Effect of pressure on the dielectric properties of ice Ih single crystals doped with NH_3 and HF, *J. Glaciology*, **21**, 85, 161–172, doi:10.1017/S0022143000033384, 1978.

Imai, M., K. Imai, C. A. Higgins, and J. R. Thieman, Comparison between Cassini and Voyager observations of Jupiter's decametric and hectometric radio emissions, *J. Geophys. Res.*, **116**, A12233, doi:10.1029/2011JA016456, 2011.

Kivelson, M. G., K. K. Khurana, and M. Volwerk, The permanent and inductive magnetic moments of Ganymede, *Icarus*, **157**, 507–522, doi:10.1006/icar.2002.6834, 2002.

Leblanc, Y., On the arc structure of the DAM Jupiter emission, *J. Geophys. Res.*, **86**, 8546–8560, 1981.

Moore, J. C., Models of radar absorption in Europan ice, *Icarus*, **147**, 292–300, doi:10.1006/icar.2000.6425, 2000.

Ono, T., A. Kumamoto, Y. Kasahara, Y. Yamaguchi, A. Yamaji, T. Kobayashi, S. Oshigami, H. Nakagawa, Y. Goto, K. Hashimoto, Y. Omura, T. Imachi, H. Matsumoto, and H. Oya, The Lunar Radar Sounder (LRS) onboard the KAGUYA (SELENE) spacecraft, *Space Sci. Rev.*, **154**, 145–192, doi:10.1007/s11214-010-9673-8, 2010.

Romero–Wolf, A., S. Vance, F. Maiwald, E. Heggy, P. Ries, and K. Liewer, A passive probe for subsurface oceans and liquid water in Jupiter's icy moons, *Icarus*, **248**, 463–477, doi:10.1016/j.icarus.2014.10.043, 2015.

Schroeder, D. M., A. Romero–Wolf, L. Carrer, C. Grima, B. A. Campbell, W. Kofman, L. Bruzzone, and D. D. Blankenship, Assessing the potential for passive radio sounding of Europa and Ganymede with RIME and REASON, *Planet. Space Sci.*, **134**, 52–60, doi:10.1016/j.pss.2016.10.007, 2016.

Siegert, M. J., R. Hodgkins, and J. A. Dowdeswell, A chronology for the Dome C deep ice–core site through radio–wave layer correlation with the Vostok ice core, Antarctica, *Geophys. Res. Lett.*, **25**, 7, 1019–1022, 1998.

Tokumaru, M., Faraday effect in the Jovian decametric radiation observed with a new radiospectrograph at Wakkanai, *J. Geomag. Geoelectr.*, **47**, 577–582, 1995.

Vance, S., M. Bouffard, M. Choukroun, and C. Sotin, Ganymede's internal structure including thermodynamics of magnesium sulfate oceans in contact with ice, *Planet. Space Sci.*, **96**, 62–70, doi:10.1016/j.pss.2014.03.011, 2014.